

(p, pn) Reactions at Proton Energies from 0.3 to 3.0 Bev*†SAMUEL S. MARKOWITZ‡ AND F. S. ROWLAND,§ *Departments of Chemistry, Princeton University, Princeton, New Jersey, and Brookhaven National Laboratory, Upton, New York*

AND

G. FRIEDLANDER, *Department of Chemistry, Brookhaven National Laboratory, Upton, New York*

(Received July 21, 1958)

Cross sections for (p, pn) reactions on N^{14} , F^{19} , Fe^{54} , Ni^{58} , Cu^{63} , Cu^{65} , Zn^{64} , Mo^{100} , and Ta^{181} have been measured at proton energies of 0.4 and 3.0 Bev. For F^{19} , Cu^{65} , Mo^{100} , and Ta^{181} cross-section measurements at several other energies between 0.3 and 3.0 Bev are reported also. Within 30%, all these (p, pn) cross sections appear to be energy-independent in this range. At a given energy the cross sections show greater variations from nucleus to nucleus than can be explained on a purely statistical picture of knock-on processes. Among the lightest nuclei (C^{12} , N^{14} , O^{16} , Fe^{19}), these variations can be correlated with the energy of the lowest lying level of the product nucleus which is stable with respect to particle emission. Among heavier nuclei this correlation disappears, and it is suggested that shell structure effects may be responsible for the fact that the (p, pn) cross sections of Cu^{63} , Cu^{65} , and Zn^{64} are about 45% higher than those of Fe^{54} and Ni^{58} . Apart from these individual variations which a statistical theory could not be

expected to reproduce, it is found that the recent Monte Carlo calculations of intranuclear cascades by Metropolis *et al.* do not even predict the right magnitude and energy dependence for the cross sections. The calculated cross sections are too small by factors of 2 to 3 at 0.4 Bev and show a decrease with increasing energy. Possible reasons for these discrepancies are sought in details of the nuclear model used in the calculations. Various mechanisms which may contribute to (p, pn) reactions are discussed. It is concluded that deuteron emission cannot contribute significantly at the energies considered. Processes involving evaporation of one of the nucleons are likely to decrease in importance with increasing energy, whereas the contribution of meson reactions, such as $(p, pn\pi^0)$, $(p, 2p\pi^-)$, etc., probably increases with energy. The observed energy independence of the cross sections may result from accidental cancellation of such opposing trends.

INTRODUCTION

PREVIOUS studies of the interactions of high-energy protons with complex nuclei have shown^{1,2} that the average energy transfers to the struck nuclei in such interactions increase markedly as the bombarding energy is increased from a few hundred to a few thousand Mev. It has been suggested^{2,3} that this increase in energy deposition may result primarily from scattering collisions and reabsorption of pions created in the intranuclear cascade, and recent Monte Carlo calculations of intranuclear cascades^{4,5} support this interpretation. In spite of this general increase in the energy deposition spectrum, the cross sections of certain simple reactions show surprisingly little energy dependence in this region.^{1,3,6-9} Among these reactions

the (p, pn) reactions are of particular interest because their cross sections are relatively high (usually several percent of the total inelastic cross section of the target nucleus) and because they have been interpreted^{7,10} as proceeding largely by the direct knock-on ejection of a neutron, at least at incident energies of 300–400 Mev.

It seemed worthwhile to investigate in more detail the energy dependence of (p, pn) cross sections above the pion production threshold to see what effect, if any, pion processes inside the nucleus have on these cross sections and whether the simple knock-on mechanism can still be used for their interpretation at these energies.

Target nuclides for this study were initially chosen to represent a wide range of nuclear sizes and included N^{14} , F^{19} , Cu^{65} , Mo^{100} , and Ta^{181} . In the course of the work it became of interest to investigate whether, at a given bombarding energy, the (p, pn) cross section varies smoothly with target mass number, as one might expect for a knock-on mechanism if shell or other nuclear structure effects can be neglected. Accordingly, the (p, pn) cross sections of a number of nuclides in a narrow mass region were measured also; these target nuclides were Fe^{54} , Ni^{58} , Cu^{63} , Cu^{65} , and Zn^{64} , and all these except for Cu^{65} were used in the form of enriched isotopes.¹¹ One of the chief criteria for the selection of targets was, of course, that the half-lives and decay properties of the product nuclides should be suitable. It should be noted that the measured Mo^{100} and Ta^{181} cross sections are not directly comparable with

* This article is based upon a dissertation submitted by Samuel S. Markowitz in partial fulfillment of the requirements for the degree of Doctor of Philosophy at Princeton University (January, 1957).

† Research supported by the U. S. Atomic Energy Commission.

‡ Present address: Department of Chemistry, University of California, Berkeley, California.

§ Present address: Department of Chemistry, University of Kansas, Lawrence, Kansas.

¹ Friedlander, Miller, Wolfgang, Hudis, and Baker, Phys. Rev. **94**, 727 (1954).

² Wolfgang, Baker, Caretto, Cumming, Friedlander, and Hudis, Phys. Rev. **103**, 394 (1956).

³ R. Wolfgang and G. Friedlander, Phys. Rev. **96**, 190 (1954), and **98**, 1871 (1955).

⁴ Metropolis, Bivins, Storm, Turkevich, Miller, and Friedlander, Phys. Rev. **110**, 185 (1958).

⁵ Metropolis, Bivins, Storm, Miller, Friedlander, and Turkevich, Phys. Rev. **110**, 204 (1958).

⁶ Friedlander, Hudis, and Wolfgang, Phys. Rev. **99**, 263 (1955).

⁷ A. A. Caretto and G. Friedlander, Phys. Rev. **110**, 1169 (1958).

⁸ Cumming, Friedlander, and Swartz, Phys. Rev. **111**, 1386 (1958).

⁹ Symonds, Warren, and Young, Proc. Phys. Soc. (London) **A70**, 824 (1957).

¹⁰ E. Belmont and J. M. Miller, Phys. Rev. **95**, 1554 (1954).

¹¹ The enriched isotopes were obtained from the Isotope Research and Production Division of the Oak Ridge National Laboratory.

the other data, because the former represents the sum of the $(p,2p)$ and (p,pn) cross sections [the $(p,2p)$ product, Nb^{99} , decays with a 2.5-min half-life to Mo^{99}], and the latter is the cross section for the production of Ta^{180m} ($t_{1/2}=8.1$ hr) only; the yield of the stable or very long-lived Ta^{180} ground state could not be measured.

EXPERIMENTAL

A. Target Irradiation

Most of the irradiations were carried out in the circulating beam of the Brookhaven Cosmotron, with protons of energies between 0.4 and 3.0 Bev. A few bombardments were performed with 0.28- and 0.38-Bev protons at the Nevis synchrocyclotron at Columbia University. The targets, whose total thickness varied between 30 and 90 mg/cm², were irradiated for periods of 5 to 60 minutes. In the Cosmotron, the targets were protected from low-energy protons by an aluminum block which was withdrawn near the end of the acceleration cycle, as previously described.²

All cross sections were measured relative to the cross section for the $\text{Al}^{27}(p,3pn)\text{Na}^{24}$ monitor reaction, which was taken to be 10.7 ± 0.6 mb over the entire energy range covered in this paper. This value is based on the absolute measurements of the $\text{C}^{12}(p,pn)\text{C}^{11}$ cross section between 0.34 and 3.0 Bev^{8,12-14} and the measured ratios of the $\text{C}^{12}(p,pn)\text{C}^{11}$, and $\text{Al}^{27}(p,3pn)\text{Na}^{24}$ cross sections.^{3,15} It is also consistent with the absolute determinations of the $\text{Al}^{27}(p,3pn)\text{Na}^{24}$ cross section at energies up to 0.66 Bev.^{12,14-16} The cross sections of these monitor reactions are discussed in detail in reference 8.

The target foils and the 21-mg/cm² aluminum monitor foil were lined up in a target holder and always irradiated with the aluminum foil "upstream" with respect to the beam direction, i.e., the aluminum was struck first by the protons. A 3.4-mg/cm² foil of polyethylene was placed between the aluminum and target foils to serve as a "catcher" which would prevent contamination of either foil by recoil nuclei from the other.

Recoil loss of (p,pn) products from the targets was checked by an experiment in which a stack of five 2.7-mg/cm² "Teflon" foils was bombarded with 3.0-Bev protons. Comparison of the F^{18} activities induced by $\text{F}^{19}(p,pn)$ reaction in the upstream, middle, and downstream foils showed that the recoil losses of F^{18} were $(3 \pm 1)\%$ in the forward direction and $< 1\%$ in the backward direction. Most of the targets were

both thicker and of higher Z than these Teflon targets; errors from recoil loss have therefore been assumed to be negligible.

The contribution of secondary particles to the observed yields of (p,pn) products and to the formation of Na^{24} in the aluminum monitor foil was made negligible by use of targets so thin that the probability for escape of secondaries produced in the target was very large. Bombardments of copper in which the target thicknesses were varied by a factor of 2 gave cross sections for the formation of Cu^{64} , which were equal within experimental error; this observation indicated that contribution of secondaries to Cu^{64} production was negligible. More careful measurements⁸ of the secondary contribution to C^{11} formation in thick plastic targets corroborate this conclusion.

Table I summarizes the composition of the targets used in the irradiations. All of the target materials were of sufficiently high purity that only negligible quantities of the observed (p,pn) products could have been formed by reactions with other elements present. The enriched isotopes were electroplated onto 0.0005-inch gold foil by standard procedures.¹⁷⁻¹⁹ Gold was used because it is insoluble in the acids used to dissolve the electroplated elements. Radioactivities induced in the gold were thus not added to the solution. Considerations of the formation cross sections and ranges of possible reaction products from gold showed that they could not contribute measurably to the observed (p,pn) formation cross sections, particularly since in the bombardments the target material was always oriented upstream from the gold.

B. Chemical Purifications

After completion of each irradiation and with the targets still fixed in the target holder, equal areas of target and monitor foils were removed by use of a metal punch. The aluminum monitor was mounted for activity measurements, and the target material was, in

TABLE I. Target composition.

Target isotope and abundance ^a	Chemical state of target material	Target thickness (mg/cm ²)
N^{14} (nat.)	Be_3N_2 powder ^b	40
F^{19} (nat.)	$(\text{CF}_2)_n$ foil	2.7
Fe^{54} (96.7%)	Fe (plated on Au)	3-4
Ni^{58} (98.4%)	Ni (plated on Au)	4-30
Cu^{63} (99.1%)	Cu (plated on Au)	3-6
Cu^{65} (nat.)	Cu metal foil	10
Zn^{64} (93.1%)	Zn (plated on Au)	3-5
Mo^{100} (nat.)	Mo metal foil	32
Ta^{181} (nat.)	Ta metal foil	10, 20

^a (nat.) indicates targets of natural isotopic composition.

^b In Be_3N_2 bombardments a 7-mg/cm² aluminum envelope was used both as container and beam monitor.

¹⁷ R. W. Dunn, University of California Radiation Laboratory Report UCRL-932, 1950 (unpublished).

¹⁸ F. Exner, J. Am. Chem. Soc. **25**, 896 (1903).

¹⁹ J. Kleinberg (editor), Atomic Energy Commission Report LA-1566, 1954 (unpublished).

¹² Crandall, Millburn, Pyle, and Birnbaum, Phys. Rev. **101**, 329 (1956).

¹³ Rosenfeld, Swanson, and Warshaw, Phys. Rev. **103**, 413 (1956).

¹⁴ J. D. Prokoshkin and A. A. Tiapkin, J. Exptl. Theoret. Phys. U.S.S.R. **32**, 177 (1957) [translation: Soviet Phys. JETP **5**, 148 (1957)].

¹⁵ Hicks, Stevenson, and Nervik, Phys. Rev. **102**, 1390 (1956).

¹⁶ L. Marquez, Phys. Rev. **86**, 405 (1952).

general, subjected to appropriate chemical purifications to insure good decontamination from other radioactive elements. Previously described procedures¹⁹⁻²¹ were usually used, but modified in some cases to facilitate rapid isolation of products with short half-lives. The following paragraphs give a brief outline of the chemical steps employed.

1. *Nitrogen and fluorine*.—No chemical purification was necessary because the activities of the (p, pn) products could be differentiated from other activities produced on the basis of half-life alone.

2. *Iron*.—Electroplated iron was dissolved away from the gold backing with HCl and purification was done by solvent extraction with isopropyl ether from 8M HCl, washing of the ether layer with 8M HCl, back-extraction into H₂O and precipitation of Fe₂O₃·*x*H₂O with NH₄OH.

3. *Nickel*.—Nickel dimethylglyoxime was precipitated from a nitric acid solution of the electroplated nickel, after the addition of cobalt "holdback" carrier, sodium citrate, and enough NH₄OH to make the solution basic. It was recycled through HCl solution, and reprecipitation of nickel dimethylglyoxime, which was then dissolved in HNO₃. After evaporation to dryness the NiO residue was redissolved in HCl, and NiS was precipitated and mounted.

4. *Copper*.—The copper foils of natural isotopic composition were dissolved in HCl plus a few drops of 30% H₂O₂; electroplated enriched copper was dissolved away from the gold backing with HNO₃. Copper sulfide was precipitated and redissolved. After a scavenging precipitation of Fe(OH)₃, the solution was acidified, CuCNS was precipitated, redissolved, and metallic Cu was precipitated by the addition of NH₄OH and heating with sodium hydrosulfite. The CNS⁻ step was eliminated when 10-min Cu⁶² was being measured.

5. *Zinc*.—Zinc was dissolved away from the gold backing with HCl, the solution adjusted to 2-3M in HCl and passed through a Dowex-A2 anion exchange column. The adsorbed zinc was eluted with NH₄OH and precipitated from hot neutral solution as ZnNH₄PO₄·H₂O for mounting.

6. *Molybdenum*.—The Mo was dissolved in H₂SO₄—HNO₃, heated to form molybdic acid, redissolved with NH₄OH, and acidified to 6M with HCl. Any reduced states were oxidized with bromine water, Fe⁺³ carrier was added, and two ethyl ether extractions were performed. The combined organic layers were washed with 6M HCl, and evaporated over H₂O to remove the ether. The solution was freed of iron by precipitation of Fe₂O₃·*x*H₂O with NH₄OH, made 0.5N in HCl, and saturated with oxalic acid. Molybdenum

alpha benzoin oxime was then precipitated, dissolved in HNO₃+HClO₄, and heated to fuming. MoO₃·*x*H₂O was precipitated with ice-cold red fuming nitric acid. Alternatively, the HNO₃—HClO₄ solution was made ammonical for the precipitation of Fe₂O₃·*x*H₂O (a scavenging step), and PbMoO₄ precipitated from the acidified filtrate. Although both procedures gave radiochemically pure 67-hr Mo⁹⁹, more consistent chemical yields and smaller self-absorption corrections were obtained for MoO₃·*x*H₂O.

7. *Tantalum*.—The tantalum foils were dissolved in HF plus HNO₃, cerium carrier was added, precipitating cerium fluoride. Zirconium and tungsten carriers were added, and BaZrF₆ was precipitated with a saturated solution of barium nitrate. Concentrated H₂SO₄ was used to precipitate excess barium, and the tantalum was then extracted from 18N H₂SO₄—0.5N HF solution with di-isopropyl ketone.²² The ketone layer was washed with 18N H₂SO₄—2N HF solution, and the Ta back-extracted with dilute boric acid solution. After addition of tungsten holdback carrier, tantalum hydroxide was precipitated with NH₄OH, and converted to tantalic acid with ice-cold red fuming nitric acid. This was ignited to Ta₂O₅, ground under acetone, and mounted.

C. Radioactivity Measurements

The aluminum monitors as well as the samples resulting from the chemical separations (or, in the cases of Be₃N₂ and "Teflon" targets, the unprocessed target materials) were mounted on 0.03-inch thick aluminum cards and covered with rubber hydrochloride films 1.2 mg/cm² thick. Radioactivity measurements were then carried out with end-window gas-flow beta proportional counters. The counting gas was a mixture of 90% argon and 10% methane. The counting efficiencies for the various nuclides were determined by methods described below.

The decay of the various radioactive nuclides was followed for many half-lives, and then the samples were dissolved and the chemical yields determined by standard spectrophotometric or polarographic techniques. By decay-curve analysis and application of corrections for length of bombardment, chemical yield, and counting efficiency, the disintegration rate of each radioactive species for an infinitely long bombardment could be determined. These saturation disintegration rates were converted to reaction cross sections by means of the proton beam intensity obtained from the yield of Na²⁴ in the aluminum monitor foil.

Since, in the present work, one of the aims was to compare cross sections for the formation of different nuclides, the detection efficiencies for the various (p, pn) products studied were determined with considerable

²⁰ M. Lindner, University of California Radiation Laboratory Report UCRL-4377, 1954 (unpublished).

²¹ W. W. Meinke, U. S. Atomic Energy Commission Report AECD-3084, 1951 (unpublished).

²² P. C. Stevenson and H. G. Hicks, Anal. Chem. **25**, 1517 (1953).

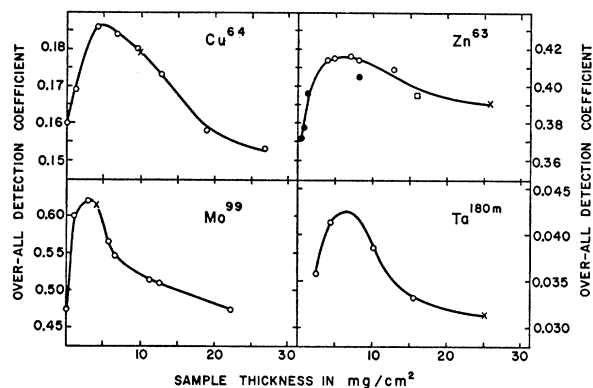


FIG. 1. Over-all detection coefficient on end-window proportional counter, as a function of sample thickness, for Cu^{64} , Zn^{63} , Mo^{99} , and Ta^{180m} . The samples were in the forms of copper metal, $\text{ZnNH}_4\text{PO}_4 \cdot \text{H}_2\text{O}$, MoO_3 , and Ta_2O_5 , respectively. The crosses represent the absolute measurements. All other points are measured relative to these. In the case of Zn^{63} , the open circles, full circles, and squares represent three different sets of relative measurements. The Ta^{180m} samples were all measured through 43 mg/cm^2 of aluminum, and the over-all detection coefficient plotted here is for those radiations which are transmitted through 43 mg/cm^2 of Al, but not through 400 mg/cm^2 of Al.

care. All of these products are β^+ or β^- emitters, and their decay properties²³ are listed in Table II.

The measured samples had varying thicknesses in the range from 2 to 20 mg/cm^2 , although for a given product all samples were of similar thickness. Self-absorption and self-scattering effects were determined in separate experiments with cyclotron- or reactor-produced samples of Cu^{64} , Zn^{63} , Mo^{99} , and Ta^{180m} . A series of samples of constant specific activity, but of different weights per unit area were prepared with each of these nuclides, and these were mounted and measured in the same manner as the samples resulting from the (p,pn) experiments. The self-absorption curves so obtained are shown in Fig. 1. It should be noted that it was not necessary to extrapolate these curves to zero samples thickness, but only to span the range of thicknesses used in the cross-section experiments. The over-all detection coefficient, defined as (counts per minute observed)/(disintegrations per minute), was then determined for each nuclide with a sample of a particular thickness by the methods described below. Since the shapes of the self-absorption curves of Cu^{64} (β^+ 0.66 Mev, β^- 0.57 Mev) and Zn^{63} (β^+ 2.23 Mev) are not grossly different, and since the detection coefficient determinations were done on samples of thicknesses similar to those of the (p,pn) products, the self-absorption corrections for Ni^{13} , Cu^{62} , and Fe^{53} were taken to be the same as for Zn^{63} , those for Ni^{57} the same as for Cu^{64} . For a given nuclide, the thicknesses of the various samples used in the cross section-measurements were sufficiently similar to each other that the detection coefficient for any sample never differed by more than

²³ Strominger, Hollander, and Seaborg, *Revs. Modern Phys.* **30**, 585 (1958).

11% from (and was usually much closer to) that of the standard sample. Thus the error introduced by errors in the self-absorption corrections made is certainly no more than a few percent. The F^{18} samples required no self-absorption correction because they were all of the thickness used in the absolute detection coefficient measurement.

The over-all detection coefficients of the β^+ emitters F^{18} , Ni^{57} , Cu^{62} , Cu^{64} , and Zn^{63} in the end-window counters were determined by annihilation radiation measurements. A sample of each of these nuclides, prepared by suitable cyclotron or reactor activation and radiochemically purified, was sandwiched between two copper sheets thick enough to absorb all the positrons, and the annihilation radiation emitted was measured with a NaI scintillation counter connected to a 100-channel pulse height analyzer. By comparison with a calibrated Na^{22} standard measured in the same manner, the positron decay rate of the sample was determined. This, together with the β^+ branching ratio (see Table II), gives the total disintegration rate of the sample. The same sample was also measured with an end-window proportional counter, in exactly the same arrangement used in the (p,pn) experiments; the over-all detection coefficient for this arrangement was thus determined, without any need for separate measurements of back-scattering, air absorption, and window absorption effects.

The Na^{22} standard sample used was prepared from a solution whose positron emission rate had been calibrated by the National Bureau of Standards. The disintegration rate of this sample was determined by β^+ -(1.28 Mev γ)²⁴ and (0.51 Mev γ)-(1.28 Mev γ) coincidence measurements also, and the results agreed within 1% with the NBS calibration, when the 10% electron capture branch²³ of Na^{22} was taken into account. To check whether the scintillation spectrometer

TABLE II. Decay properties of the observed (p,pn) products.

Product nuclide	$T_{1/2}$		% Decay			E_{\max} β^+ or β^- (Mev)
	from Strominger <i>et al.</i> ^a	observed ^b	β^+	EC	β^-	
Ni^{13}	10.1 min	(10 min)	100	1.2
F^{18}	112 min	112 ± 1 min	97	3	...	0.65
Fe^{53}	8.9 min	9.3 ± 0.4 min	98	2 ^c	...	2.6
Ni^{57}	36 hr	35.9 ± 0.4 hr	50	50	...	0.84
Cu^{62}	9.73 min	(10 min)	98	2 ^c	...	2.91
Cu^{64}	12.80 hr	12.8 ± 0.1 hr	19	43	38	$0.66\beta^+$, $0.57\beta^-$
Zn^{63}	38.3 min	38.6 ± 0.8 min	93	7	...	2.23
Mo^{99}	67 hr	67.0 ± 0.5 hr	100	1.2
Ta^{180m}	8.2 hr	8.3 ± 0.2 hr	...	79	21	0.7

^a See reference 23.

^b The half-lives listed in parentheses in this column are assigned values used in the analysis of the decay curves. The errors given are the standard deviations of the means of the half-life determinations from the various bombardments. The number of observations varied between four for Fe^{53} and twenty for Cu^{64} and Mo^{99} .

^c The electron capture branching ratios of Fe^{53} and Cu^{62} are theoretical estimates taken from *Nuclear Level Schemes, A=40-A=92*, compiled by Way, King, McGinnis, and van Lieshout, Atomic Energy Commission Report TID-5300 (U. S. Government Printing Office, Washington, D. C., 1955).

²⁴ The results of the β^+ - γ measurements were kindly made available by Dr. M. L. Perlman and Dr. J. B. Cumming.

detection efficiency varied with the maximum β^+ energy because of differences in the annihilation volume in the copper absorber, the $\text{Zn}^{63}/\text{Na}^{22}$ ratios were measured in several different geometries. No significant differences were found and it was thus concluded that, at the source-to-crystal distances used, the solid angle subtended by the crystal with respect to the annihilation volume was essentially independent of β^+ energy.

The positron detection efficiencies for N^{13} and Fe^{53} were not directly determined. That of Fe^{53} ($E_{\text{max}}=2.5$ Mev) was taken to be the same as that of Zn^{63} ($E_{\text{max}}=2.36$ Mev), that of N^{13} ($E_{\text{max}}=1.2$ Mev) the same as that of Cu^{61} ($E_{\text{max}}=1.2$ Mev) which, because of its longer half-life, was more convenient than N^{13} for this efficiency determination.

The absolute disintegration rate of a Mo^{99} sample prepared by the $\text{Mo}^{98}(n, \gamma)$ reaction was determined by three different methods and the activity of the same sample was measured on the end-window counter, thus giving the over-all detection coefficient in that counter. One method consisted in a measurement of the 140-keV gamma ray of the Tc^{99m} daughter in equilibrium with Mo^{99} by means of a well-type 4π scintillation counter connected to a single-channel pulse-height analyzer. According to the published decay schemes²³ of Mo^{99} and Tc^{99m} , 89% of the Mo^{99} disintegrations are accompanied by emission of 140-keV quanta (not coincident with other γ rays); the detection efficiency of the 4π scintillation counter for 140-keV quanta was 97%. In a separate measurement with the same scintillation counter, but without pulse height analysis, the total gamma-ray rate of the sample was measured; the total disintegration rate was computed by division of this rate by 1.03—the number of noncoincident gamma quanta per Mo^{99} decay.²³ In a third determination, the activity of a 50- μg aliquot of the sample was measured in a 4π beta counter. The three measurements agreed with each other within a 5% spread.

A Ta^{180m} sample for calibration measurements was prepared by $\text{Ta}^{181}(n, 2n)$ reaction; its disintegration rate was determined by 4π scintillation counting of the K x-rays emitted following its decay. From the published decay scheme,²³ the L/K capture ratio,²⁵ and the fluorescence yield²⁶ it was concluded that 68% of the Ta^{180m} decays are accompanied by K x-ray emission. The detection efficiency of the 4π scintillation counter for 56-keV x-rays was taken as 94%, the losses being due to absorption in the covering of the crystal.

An additional complication in the end-window counter measurements of Ta^{180m} produced by high-energy (p, pn) reaction was the presence of 8.0-hr Ta^{176} in the same samples, formed via a $(p, p5n)$ reaction. This isotope decays by electron capture, with the emission of x-rays, conversion electrons (up to ~ 0.2 Mev) and γ rays, whereas 21% of Ta^{180m} decays

TABLE III. Isotopic cross sections for (p, pn) reactions at high energies (millibarns).

Target nuclide	Proton energy (Bev)														
	0.28	0.38	0.4	0.6	0.8	1.0	1.2	1.3	1.4	1.6	1.9	2.2	2.6	2.9	3.0
N^{14}			5.6												3.1
F^{19}	28	27	26	26	25	21	23		24	24		27			28
Fe^{54}			48												28
Ni^{58}			45												47
Cu^{63}			52												42
Cu^{65}			47												39
Cu^{65}	69	68	67	51	60	56		59		62		58	54	58	62
Zn^{64}		83	73		60							65		65	71
Zn^{64}			71												73
Mo^{100a}	79	65	66	81	60	67		66		73	71	73	81	73	82
Mo^{100a}			79		61			76				72	75	72	63
Ta^{181b}	44	62	46			36						25	42	46	47
Ta^{181b}		53										33			

^a Includes contribution from $\text{Mo}^{100}(p, 2p)$ reaction.

^b Does not include cross section for production of Ta^{180} ground state.

proceed by β^- emission ($E_{\text{max}}=0.71, 0.61$ Mev). Discrimination against Ta^{176} was thus achieved by use of a 43-mg/cm² aluminum absorber to cut out the conversion electrons and reduce the L x-ray contribution. The small fraction ($\sim 4\%$) of the counts in the end-window counter due to K x-rays and γ rays was determined for each (p, pn) -produced sample by absorption of the β^- component in ~ 400 mg/cm² of aluminum. The measurement of the over-all detection coefficient with the Ta^{180m} calibration sample was, of course, also carried out under the 43-mg/cm² absorber.

RESULTS

The individual (p, pn) cross sections are shown in Table III, and the excitation functions for F^{19} , Cu^{65} , Mo^{100} , and Ta^{181} are given graphically in Figs. 2 and 3. The root-mean-squares errors resulting from uncertainties in counting efficiencies, chemical yields, decay curve resolutions, and branching ratios are estimated to be $\pm 10\%$ except in the cases of N^{13} and Ta^{180} , where they are thought to be $\pm 20\%$ and $\pm 25\%$, respectively. These errors do not include the uncertainty of $\pm 6\%$ in the 10.7-mb cross section⁸ for the $\text{Al}^{27}(p, 3pn)\text{Na}^{24}$ reaction, an uncertainty which of course does not affect comparisons of cross sections at any given energy.

From the shapes of the excitation functions it can be seen that there is little change in the (p, pn) cross sections in the range 0.3 to 3.0 Bev. The cross sections for the (p, pn) reactions on F^{19} and Cu^{65} (Fig. 2) and also on C^{12} (from references 3, 8, 9, 12–14) decrease slightly from 0.3 to 1 Bev and then remain fairly constant from 1 to 3 Bev. The cross sections for N^{14} , Fe^{54} , Ni^{58} , Cu^{63} , and Zn^{64} are nearly the same at 0.4 Bev as at 3.0 Bev, the only energies for which they have been measured in the present study. The shapes of the excitation functions for production of Mo^{99} and Ta^{180m} are similar to those for the (p, pn) reactions on C^{12} , F^{19} , and Cu^{65} , although, as mentioned in the Introduction,

²⁵ M. E. Rose and J. L. Jackson, Phys. Rev. **76**, 1540 (1949).

²⁶ Broyles, Thomas, and Haynes, Phys. Rev. **89**, 715 (1953).

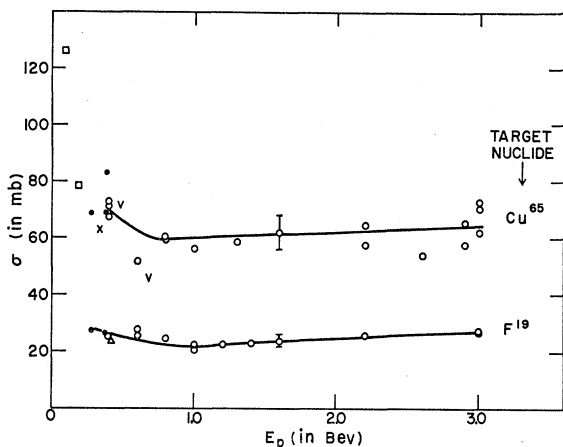


FIG. 2. Excitation functions for the reactions $F^{19}(p,pn)F^{18}$ and $Cu^{65}(p,pn)Cu^{64}$. \circ This paper—Cosmotron data. \bullet This paper—Nevis cyclotron data. \triangle Marquez, reference 16. \square C. H. Coleman and H. A. Tewes, Phys. Rev. **99**, 288 (1955). ∇ Vinogradov *et al.*, *Proceedings of the Conference of the Academy of Sciences of the U.S.S.R. on the Peaceful Uses of Atomic Energy, Moscow, July 1-5, 1955* (Akademiia Nauk, S.S.S.R., Moscow, 1955), session of Division of Chemical Sciences, p. 132 [English translation by Consultants Bureau, New York: U. S. Atomic Energy Commission Report Tr-2435 (1956), Part 2, p. 85]. \times Batzel, Miller, and Seaborg, Phys. Rev. **84**, 671 (1951).

the Mo^{99} yield includes the $p,2p$ reaction on Mo^{100} and the Ta^{180m} yield represents only part of the $Ta^{181}(p,pn)$ cross section. The cross sections for (p,pn) reactions reported here thus are nearly energy-independent in the BeV region over a wide range of nuclear sizes. Caretto and Friedlander,⁷ however, have measured a decrease of a factor of about 2.8 in the $Ce^{142}(p,pn)Ce^{141}$ cross section from 0.4 BeV (86 mb) to 1.0 BeV (31 mb), followed by a nearly constant value from 1 to 3 BeV. Burcham, Symonds, and Young²⁷ reported a dip of

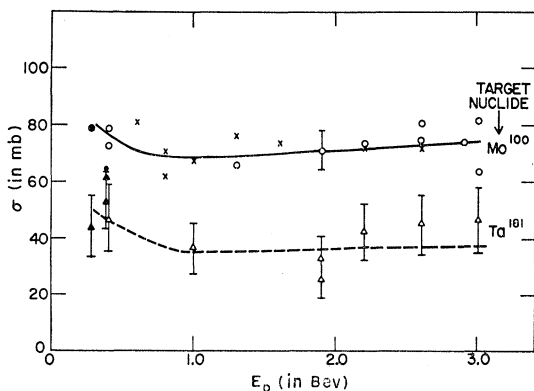


FIG. 3. Excitation functions for the reactions $[Mo^{100}(p,pn)Mo^{99}$ plus $Mo^{100}(p,2p)Mo^{99}]$ and $Ta^{181}(p,pn)Ta^{180m}$. The open circles and triangles represent Cosmotron data, the full circles and triangles are data obtained with the Nevis cyclotron. The crosses are measurements in which Mo was in the form of $PbMoO_4$, rather than MoO_3 .

²⁷ Burcham, Symonds, and Young, Proc. Phys. Soc. (London) **A68**, 1001 (1955).

about 30% in the $C^{12}(p,pn)$ cross section near 650 Mev, followed by a maximum near 800 Mev. Symonds, Warren, and Young⁹ report a peak at about 750 Mev in the $F^{19}(p,pn)$ cross section, which is not found in the present work, perhaps because our bombarding energies were not closely enough spaced. The same authors quote values of 9 to 12 mb for the $N^{14}(p,pn)$ cross section between 0.4 and 1.0 BeV, considerably higher than the 6 ± 1 mb value at 0.4 BeV found here.

DISCUSSION

There are three general conclusions that can be drawn from these experiments relative to (p,pn) reactions at high energies:

- (1) All (p,pn) cross sections measured are essentially constant in the energy region 1.0 to 3.0 BeV, and most do not decrease very much from 0.3–1.0 BeV.
- (2) Cross sections for light nuclides differ considerably from one another in the BeV energy region. In addition to the 5 ± 1 mb value for N^{14} and the 25 ± 3 mb value for F^{19} reported here over the entire energy range, (p,pn) cross sections have also been published for C^{12} (26 ± 1 mb at 2 to 3 BeV),⁸ and for O^{16} (37 mb at 1.0 BeV).⁹
- (3) The cross sections in the narrow mass region $54 \leq A \leq 65$ appear to fall into two groups, those for Cu^{63} , Cu^{65} , and Zn^{64} being about 45% higher than those for Fe^{54} and Ni^{58} .

Possible Mechanisms

The radiochemically observed products of “ (p,pn) ” reactions could be formed by a variety of processes.

(a) A pure knock-on process for a (p,pn) reaction involves the collision of the incident proton with a neutron, followed by the escape of both collision partners without additional interactions. Further, the neutron must not be bound so tightly that its removal leaves the nucleus sufficiently excited to evaporate an additional nucleon.

(b) Alternatively, the incident proton may make an elastic collision with a nucleon in such a way that one collision partner leaves with almost the full amount of kinetic energy available. The other partner distributes its energy in the nucleus in subsequent collisions, and eventually one additional nucleon evaporates. For this type of process (knock-on followed by evaporation) to be probable, the initial collision has to deposit about 10 to 20 Mev in the nucleus.

(c) At energies above the pion production threshold, additional mechanisms become possible, such as the reactions $(p,2p\pi^-)$, $(p,pn\pi^0)$, $(p,pn\pi^+\pi^-)$, etc. with all partners escaping. Again, all the escaping particles may originate in the initial collision, or one of the nucleons could be evaporated, following the deposition of a small amount of excitation.

(d) The emission of a deuteron, rather than a proton

and a neutron, would lead to the same product. (*p,d*) reactions proceeding by a pickup process are well known at lower energies.

It is most unlikely that the last process can contribute significantly in the energy region of interest. The direct (*p,d*) pickup reaction falls off very rapidly with increasing energy, probably²⁸ as E^{-6} , and has been shown²⁹ to be unimportant even at 300 Mev. Deuterons emitted from nuclei bombarded with 300-Mev nucleons were found²⁹ to have angular distributions consistent with an indirect pickup process³⁰ in which an initial scattering collision is followed by a pickup reaction for one of the collision partners. The wide-angle scattering events which account for the bulk of the observed deuterons must be accompanied by the emission of at least one additional nucleon and thus do not lead to “(*p,pn*)” products.

Comparison with Monte Carlo Cascade Calculations

Attempts to date to compute cross sections for high-energy nuclear reactions have generally considered the nucleus as a degenerate Fermi gas. The approach has been to apply Monte Carlo methods to follow the course of the intranuclear cascade that develops as the result of an initial nucleon-nucleon collision. Recent calculations of this type by Metropolis *et al.*^{4,5} predict quite well the over-all yield distribution of spallation products of copper produced at several proton energies and give generally satisfactory agreement with the observed number distributions, energy spectra, and angular distributions of emitted particles found in various experiments with incident protons and pions.

Comparison of these calculations with the present experimental data indicates poor agreement with respect to both the magnitude and energy dependence of the (*p,pn*) cross sections.

For this comparison, any cascade product of the type Z^{A-1} with excitation energy less than 10 Mev was considered a “(*p,pn*)” product from target Z^A . In addition, cascade products Z^A and $(Z+1)^A$ with excitation energy between 10 and 22 Mev were considered as potential contributors to the “(*p,pn*)” products by evaporation of a neutron or proton, respectively. Neutrons and protons were assigned equal probability for evaporation. Since the number of evaporation events was always smaller than the direct cascade events, more accurate relative probabilities for neutron and proton evaporation would have little effect on the total of “(*p,pn*)” events. Similarly, different excitation energy cutoff values (e.g., 8 and 20 Mev) do not affect this comparison significantly. On the basis of this analysis, the calculations of Metropolis *et al.* lead to the (*p,pn*) cross sections shown

TABLE IV. (*p,pn*) Cross sections (in mb) predicted by the Monte Carlo calculations of Metropolis *et al.*^a

Target	Proton energy			
	460 Mev	690 Mev	940 Mev	1840 Mev
Al ²⁷	20±3			4.0±1.4
Cu ⁶⁴	24±5	16±5	14±4	7 ±3
Ru ¹⁰⁰	26±6		15±5	3 ±3
Ce ¹⁴⁰	19±6			10 ±5
Bi ²⁰⁹	18±6		11±5	7 ±5
U ²³⁸	29±8		7±5	3 ±3

^a Each error quoted in this table is based on the square root of the number N of observed cascades interpreted as (*p,pn*) events. This procedure was followed for the sake of simplicity although arguments can be given for using, in the case of a small number of events, the square root of $N+1$. The conclusions would not be significantly changed if the latter practice were followed.

in Table IV. Although the statistical accuracy of these data is poor, it is sufficient to show that the calculated cross sections are substantially lower than the observed values in the same mass region, and that the calculations predict a decrease in (*p,pn*) cross sections with increasing bombarding energy, a prediction which is not in accord with the present observations.

It has been suggested^{4,5,7} that the underestimate of the (*p,pn*) cross section by the Monte Carlo calculation results from the assumption of a constant nuclear density up to a sharp boundary. The (*p,pn*) reactions largely result from single nucleon-nucleon encounters with the escape of both collision partners, and such events are most probable near the nuclear surface. Therefore, a more realistic nuclear model with a diffuse edge might be expected to lead to higher predicted (*p,pn*) cross sections. It is not clear, however, that such a modification of the model would raise the predicted values sufficiently, nor that it would remove the energy dependence of the cross sections in the present calculations.

On the basis of the present model or the modification suggested above, an energy-independent cross section is likely to arise only through some compensation of effects. The calculations of Metropolis *et al.* indicate that knock-on followed by evaporation (mechanism *b*) contributes about one tenth to one third of the calculated cross section at 0.46 Bev, but has essentially disappeared at 1.84 Bev. On the other hand, “(*p,pn*)” reactions involving pions (mechanism *c*) are negligible at 0.46 Bev, but contribute about half the calculated events at 1.84 Bev. Again, the computed contributions of these various mechanisms would change with the introduction of a diffuse nuclear boundary, but the trends with energy should remain qualitatively the same.

Variation of (*p,pn*) Cross Sections with *A*

A model based on a degenerate Fermi gas of nucleons should lead to a smooth variation of cross section with the size of the target nucleus. The observed cross sections show a greater fluctuation for different nuclides than such a model can predict.

²⁸ J. Heidman, Phys. Rev. **80**, 171 (1950).

²⁹ W. Hess and B. Moyer, Phys. Rev. **101**, 337 (1956).

³⁰ B. H. Bransden, Proc. Phys. Soc. (London) **A65**, 738 (1952).

TABLE V. Correlation of light-element (p, pn) cross section at 0.4 Bev with separation energy of most loosely bound particle.

Target nuclide	Lowest separation energy in (p, pn) product ^a (Mev)	Separation reaction	Cross section of (p, pn) reaction (in mb) at 0.4 Bev
N ¹⁴	1.95	N ¹³ → C ¹² +H ¹	6
F ¹⁹	4.41	F ¹⁸ → N ¹⁴ +He ⁴	25
O ¹⁶	7.35	O ¹⁵ → N ¹⁴ +H ¹	31 ^b
C ¹²	7.55	C ¹¹ → Be ⁷ +He ⁴	33 ^c

^a Obtained from the mass data of A. H. Wapstra, *Physica* 21, 367 (1955).

^b From reference 9.

^c Interpolated from references 12 and 13; see also references 8 and 9.

Among the observed (p, pn) cross sections, that for N¹⁴ is strikingly low. Cross sections for the production of N¹³ have previously been found to be abnormally low in high-energy proton bombardments of aluminum,^{6,31} fluorine,⁹ and oxygen.⁹ Following a suggestion by D. H. Wilkinson, these low values have been ascribed⁶ to the fact that all of the excited states of N¹³ are unstable with respect to proton emission. The observed cross section for the N¹⁴(p, pn)N¹³ reaction must then correspond to the formation of N¹³ in its ground state.

In view of the N¹⁴ results it seemed of interest to examine any possible correlation between the other (p, pn) cross sections and the separation energies of the most loosely bound particles (protons, neutrons, or alpha particles) in the product nuclei. Among the light elements there appears to be such a correlation, as shown in Table V, whereas there is no correlation between cross section and mass number. The same observation has recently been made by Symonds *et al.*⁹

For the (p, pn) reactions investigated in the region $54 \leq A \leq 65$, there is no simple correlation between cross sections and separation energies of nucleons and alpha particles in the (p, pn) products such as seems to exist among the light elements. In fact, the minimum separation energies for Fe⁶³ and Ni⁵⁷ are higher than for Cu⁶², Cu⁶⁴, and Zn⁶³ whereas the (p, pn) cross sections for Fe⁵⁴ and Ni⁵⁸ are the lowest measured in this region. There also is no apparent relation between neutron binding energy in the target nucleus and (p, pn) cross section, and this is hardly surprising for a high-energy process. The five nuclides investigated in this mass region all have even numbers of neutrons, so that one cannot learn anything from the present data about the relative ease of removing a paired or an unpaired neutron.

The only promising approach to finding some correlation between the (p, pn) cross sections and some other nuclear properties appears to lie in the direction of

³¹ Chackett, Chackett, Reasbeck, Symonds, and Warren, *Proc. Phys. Soc. (London)* A69, 43 (1956).

shell structure effects. Both Fe⁵⁴ and Ni⁵⁸ are magic number nuclei (with 28 neutrons and 28 protons, respectively) and as such may have abnormally small nuclear radii. Such a radius shrinkage (of 1 to 9%) has been suggested on the basis of alpha-decay data by Perlman, Ghiorso, and Seaborg³² at the magic numbers 82 and 126. Such a purely geometric effect, however, is almost certainly not large enough to explain the magnitude (~45%) of the observed depression of the (p, pn) cross section at Fe⁵⁴ and Ni⁵⁸.

More subtle shell structure effects on (p, pn) cross sections may be expected if neutrons in different angular momentum states have different radial distributions, those with higher angular momenta having relatively greater probabilities of being near the nuclear surface. Perhaps the fact that Cu⁶³, Cu⁶⁵, and Zn⁶⁴ have (p, pn) cross sections of 65 to 70 mb has something to do with the $f_{7/2}$ neutrons present in all these nuclei, whereas Ni⁵⁸ (with a cross section of 40-45 mb) presumably has its most loosely bound neutrons in $p_{3/2}$ levels. The possibility of a more quantitative correlation between the magnitude of the (p, pn) cross section and nuclear level structure has been pointed out by Grover.³³ He considers as available for (p, pn) reactions only those neutrons which are in levels sufficiently high so that removal of a neutron does not leave enough excitation energy in the nucleus for evaporation of an additional particle; on this basis he can account for the relative magnitudes of all (p, pn) cross sections above 0.4 Bev measured to date. Similar considerations have been given by Benioff.³⁴

ACKNOWLEDGMENTS

It is a pleasure to thank Professor J. M. Miller and Dr. J. B. Cumming for many helpful discussions. The help of Dr. K. Rowley, Mr. M. Slavin, Dr. R. Stoenner, and Miss E. Norton in performing chemical analyses, and that of Mrs. R. Chertok and Mrs. G. Thieben in the radioactivity measurements is gratefully acknowledged. Mr. E. Nielsen's and Mr. A. Weinstein's assistance with instrumentation problems was most helpful. Dr. D. Greenberg of Columbia University, Mr. A. Emann of Princeton University, and Dr. C. P. Baker of Brookhaven kindly carried out cyclotron bombardments, and the operating personnel of the Cosmotron deserve special thanks for their patient cooperation during many irradiations. One of us (S.S.M.) gratefully acknowledges financial aid in the form of a LeRoy McKay Fellowship (1954-1955) and a Charlotte Elizabeth Procter Fellowship (1955-1956).

³² Perlman, Ghiorso, and Seaborg, *Phys. Rev.* 77, 26 (1950).

³³ J. R. Grover (private communication).

³⁴ P. Benioff (private communication).